Hindawi
Advances in Materials Science and Engineering
Volume 2018, Article ID 8614740, 10 pages
https://doi.org/10.1155/2018/8614740

Research Article

Behavior of Chinese Dahurian Larch Wood after High-Temperature Exposure: Degradation of Mechanical Properties and Damage Constitutive Model

Qifang Xie,[1] **Lipeng Zhang**,[1] **Zhenglei Yang**,[2] **Long Wang**,[1] **and Yaopeng Wu**[1]

[1]*State Key Laboratory of Green Building in Western China, Xi'an University of Architecture and Technology, Xi'an, Shaanxi 710055, China*
[2]*Beijing Institute of Architectural Design, Beijing 100045, China*

Correspondence should be addressed to Qifang Xie; xieqfgh@xauat.edu.cn

Received 12 May 2018; Revised 10 July 2018; Accepted 19 July 2018; Published 12 September 2018

Academic Editor: Andres Sotelo

Wood has been extensively used in Chinese ancient buildings, and it is important to clearly understand the mechanical properties of wood after exposure to elevated temperatures. In this paper, three kinds of tests with 102 clear wood specimens fabricated with Chinese Dahurian larch for each kind of test were conducted. The residual compressive strength, tensile strength, and shear strength parallel to grain of specimens after exposure to different temperatures (100°C, 150°C, 200°C, and 250°C) with various exposure times (15 min, 30 min, and 45 min) and different cooling methods (natural cooling and water cooling) were obtained. Results indicate that exposure to elevated temperatures causes great degradation of compressive strength, tensile strength, and shear strength parallel to grain. When the exposure temperatures exceed 200°C, the relative compressive strength, tensile strength, and shear strength parallel to grain decrease greatly with the increase of exposure time. The residual compressive strength, tensile strength, and shear strength of specimens after water cooling are lower than that after natural cooling. Exposure temperatures also have a great impact on the weight loss and color change of wood. Based on the test data, degradation models for the residual compressive strength, tensile strength, and shear strength of wood were developed. Furthermore, the damage constitutive model of compressive (CDM_C) and tensile (CDM_T) parallel to grain was established and validated reasonably by tests.

1. Introduction

In China, Japan, and Korea, ancient timber buildings are extensively used and many have been selected as world material and cultural heritages [1]. Due to the combustible nature of wood coupled with the lack of the fire resistance design, traditional timber structures are made vulnerable to fire, which usually exerts devastating impact on the load-bearing capacity of them [2]. As a consequence, timber structural engineers are always facing the challenges of evaluating and designing repair plans for such structures, especially for those which survive from a fire without severe damages and have not been weakened too much. As for precious heritage timber buildings, keeping them as what they are is required by the protection standard GB 50165 [3]. Fortunately, it is proved possible by the facts that wood members are usually able to maintain a substantial part of the load-bearing capacity due to an insulating char layer when initially exposed to fire (Figure 1) [4]. For instance, a fire-damaged timber beam in Guardian Angels Church (in America), survived from a fire in 1902, was reused [5], as shown in Figure 2. Therefore, correct mechanical properties evaluation of fire-damaged wood is of great significance [6].

The sketch map of the residual and effective cross section definition of a fire-damaged timber member (Figure 1) illustrates the wood damage mechanism in fire [7]. It can be seen that the cross section of fire-damaged wood is mainly composed of the charring region, high-temperature decomposition region, and central intact region in light of the surface temperature [8]. Existing studies have shown that wood begins to char at 300°C and forms the charring region [9], which would later completely lose the carrying capacity [10]. Therefore, the

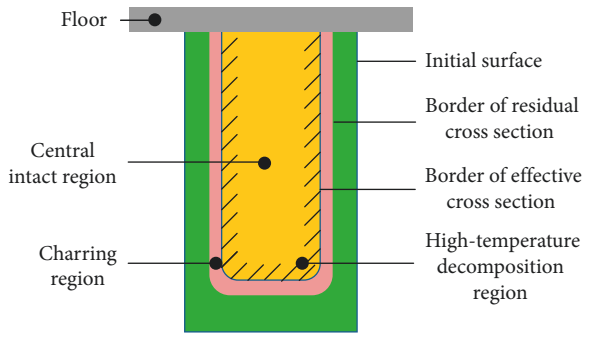

Figure 1: Sketch map of charring wood beam after exposed to fire from three sides.

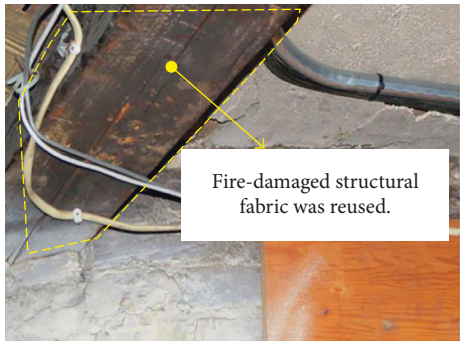

Figure 2: Charred heavy timber beam surviving from 1902 fire in Guardian Angels Church and reused in the rebuild [5].

calculation method of charring depth is of high significance and has received sufficient consideration. White and Nordheim [11] modeled the charring rate and residual strength of solid wood when exposed to fire. Firmanti et al. [12] examined the relationship between stress level and the fire resistance of lumber and concluded that the fire performance under applied load could be predicted by using simplified fire-testing methods. Xu et al. [13] experimentally studied the mechanical behaviors of timber beams exposed to three-side fire. Chen et al. [14] compared the calculation methods for fire rate of timber beams Eurocode, American code, Australia code, and Canada code and found that Australia code prediction including the density effect of wood species was more closer to test results. Wen et al. [15] established an integral charring rate model for commercial Chinese timber species based on thermodynamic equations.

Mechanical properties of fire-damaged wood have also been extensively investigated due to their important roles in the correct prediction of the residual load carrying capacity. Östman [16] reported that temperature increase would lead to a more or less linear decrease in the tensile strength and elastic modulus up to 200°C. Above 200°C, a more rapid decrease followed due to thermal softening. Winandy and Lebow [17] reported that the modulus of rupture (MOR) of wood decreased as temperature increased significantly, but the modulus of elasticity (MOE) did not show significant degradation. Bekhta and Niema [18] have also studied the effect of elevated temperature on mechanical properties of wood. Zeeland et al. [19] developed a model to predict the residual compressive strength parallel to grain for dimension lumber subjected to elevated temperatures. Goodrich et al. [20] have conducted an experimental study into thermal softening and thermal recovery of the compressive strength of structural balsa wood and revealed that when balsa is heated to 250°C or higher, the postheating strength properties would be reduced significantly by decomposition processes of all wood constituents, which irreversibly degrade the wood microstructure. Hall [21] investigated the fire behaviors of tropical wood species and subsequently assessed the fire resistance of elements made of this material. Li [22] summarized the physical and mechanical properties of wood by comparing the experimental results of Eurocode 5 [7], Östman [16], Preusser [23], Schaffer [24], Lie [25], Janssens [26], Thomas [27], Konig and Walleij [28], and Knudson and Schniewind [29].

In summary, abundant achievements about the mechanical properties of fire-damaged wood have been achieved. However, they are mainly focused on foreign tree species, which can not be directly utilized for domestic application. In addition, the existing researches did not take into consideration the influences of the exposure time to fire on the mechanical properties of fire-damaged wood. In practical structural engineering, fire on structures is usually extinguished by fire-fighting means (water or dry ice), which should also be considered. In this paper, the mechanical properties of wood exposure to elevated temperatures such as the compressive strength, the tensile strength, and shear strength parallel to grain have been experimentally studied. The purposes included are as follows:

(1) Study the effect of exposure temperature, exposure time, and cooling methods after high-temperature exposure on the above three mechanical properties, respectively.

(2) Develop proper prediction models based on test results for degradation of the above three mechanical properties, respectively.

(3) Establish a damage constitutive model of high temperature-damaged wood to reflect the deformation characteristics.

2. Materials and Methods

2.1. Specimen Production. The Chinese Dahurian larch (*Larix gmelinii*) has been frequently used in the ancient Chinese timber buildings, and commercially available Chinese larch log wood ($D = 220\sim250$ mm) was selected for this study. Small clear specimens without knots and decay were cut according to *the Method of Sample Logs Sawing and Test Specimens Selection for Physical and Mechanical Tests of Wood* [30]. All the specimens were made by a professional carpenter.

Test 1 aims at determining the compressive strength parallel to grain. Dimension of such specimens is 20 mm × 20 mm × 30 mm with 30 mm in the longitude direction. All samples were fabricated according to *the Method of Testing in Compressive Strength Parallel to Grain of Wood* [31].

Test 2 aims at obtaining the tensile strength parallel to grain. Detailed dimensions of specimens are shown in Figure 3 according to *the Method of Testing in Tensile Strength Parallel to Grain of Wood* [32].

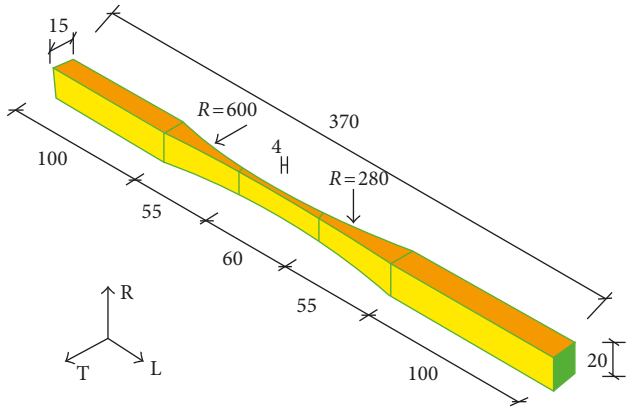

Figure 3: Details of specimens for tensile strength parallel to grain of wood (unit: mm).

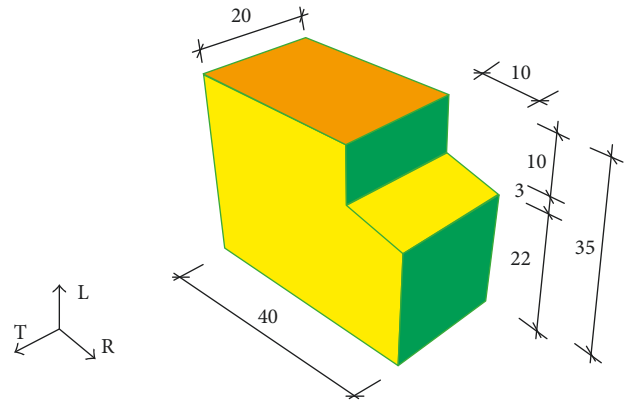

Figure 4: Details of specimens for shear strength parallel to grain of wood (unit: mm).

Test 3 aims at determining the shear strength parallel to grain. The dimension of specimens is shown in Figure 4 according to *the Method of Testing in shearing Strength Parallel to Grain of Wood* [33].

Each test has one hundred and two specimens and is classified into three groups (i.e., Group A, Group B, and Group C). Table 1 gives a summary of the details of the specimens for each test. Specimens for each test are identified by the notation $W-T*E*-$NC/WC, where "W" donates the wood specimen, "T" indicates the exposure temperature (T100 means that the exposure temperature is 100°C), "E" gives the exposure time (E15 means that the exposure time is 15 min), and "NC/WC" is the cooling method after temperature ("NC" and "WC" indicate natural cooling and water cooling, respectively). For instance, "W-T200E30WC" means that the specimen for each test is exposed to 200°C temperature with 30 min exposure time and then cooled with water. Here, the exposure time is a time period after the desired temperature is reached. Some of the specimens are shown in Figure 5.

2.2. Thermal Treatment. All the specimens for each test were placed into a ZWL-14-8Y electric furnace. For each temperature, a separate furnace run was scheduled. During the elevated temperature process, the internal temperature of the furnace increased to the given value at a rate of 5°C/min, and then the given exposure temperature was maintained for the certain exposure time (Table 1). Once the specimens were taken out of the furnace, some specimens were cooled to room temperature in air and others to room temperature with water. To reduce the water content of the water cooled specimens, they were dried in a conditioning chamber maintained at 60°C for 24 h.

2.3. Weight and Moisture Content Measuring. The weight and moisture content of all specimens were measured before heating and after cooling to room temperature by an electronic scale, with a calibrated capacity of 100 g and a precision of 0.001 g.

2.4. Test Procedures. All of the tests were conducted on a DNS-300 universal timber testing machine in the laboratory of Xi'an University of Architecture and Technology. Specimens of Test 1 and Test 2 were, respectively, loaded at a compressive and tensile rate of 0.2 mm/min up to failure. The compressive strength parallel to grain was calculated by

$$\sigma_c = \frac{P_{c,max}}{b_c t_c}, \tag{1}$$

where σ_c represents the compressive strength parallel to grain, $P_{c,max}$ is the maximum compressive load, and b_c and t_c are the width and thickness of the compressive specimens.

The tensile strength parallel to grain of wood was calculated by

$$\sigma_t = \frac{P_{t,max}}{b_t t_t}, \tag{2}$$

where σ_t represents the tensile strength parallel to grain, $P_{t,max}$ is the maximum tensile load, and b_t and t_t are the width and thickness of the middle section of the tensile specimens.

Specimens of Test 3 were loaded at a rate of 0.1 mm/min up to failure in compressive using special ancillary equipment (Figure 6). The shear strength parallel to grain of wood was calculated by

$$\tau = \frac{0.96 P_{\tau,max}}{b_\tau l_\tau}, \tag{3}$$

where $P_{\tau,max}$ represents the maximum shear load and $b_\tau = 25$ mm and $l_\tau = 10$ mm are the width and thickness of the shear section of shear specimens.

Water content of the wood material greatly affects their property. For comparison convenience, test results at the experimental water level were adjusted to equivalent values at water content 12% according to GB 1935-91, GB 1938-91, and GB 1937-91 by the following equation:

$$\begin{aligned} \sigma_{c,12} &= \sigma_c [1 + 0.05(\omega - 12)], \\ \sigma_{t,12} &= \sigma_t [1 + 0.0015(\omega - 12)], \\ \tau_{12} &= \tau [1 + 0.03(\omega - 12)], \end{aligned} \tag{4}$$

where $\sigma_{c,12}$, $\sigma_{t,12}$, and τ_{12}, respectively, represent the compressive strength, tensile strength, and shear strength parallel

Table 1: Details of wood specimens for each test.

Group	Notation	Number of specimens	Exposure temperature (°C)	Exposure time (min)	Cooling method
	W-R	6	25	—	—
Group A	W-T100E15NC	6	100	15	NC
	W-T150E15NC	6	150	15	NC
	W-T200E15NC	6	200	15	NC
	W-T250E15NC	6	250	15	NC
Group B	W-T100E30NC	6	100	30	NC
	W-T150E30NC	6	150	30	NC
	W-T200E30NC	6	200	30	NC
	W-T250E30NC	6	250	30	NC
	W-T100E30WC	6	100	30	WC
	W-T150E30WC	6	150	30	WC
	W-T200E30WC	6	200	30	WC
	W-T250E30WC	6	250	30	WC
Group C	W-T100E45NC	6	100	45	NC
	W-T150E45NC	6	150	45	NC
	W-T200E45NC	6	200	45	NC
	W-T250E45NC	6	250	45	NC

Note. NC, natural cooling; WC, water cooling.

(a) (b) (c)

Figure 5: Specimens for three tests: (a) compressive specimens; (b) tensile specimens; (c) shear specimens.

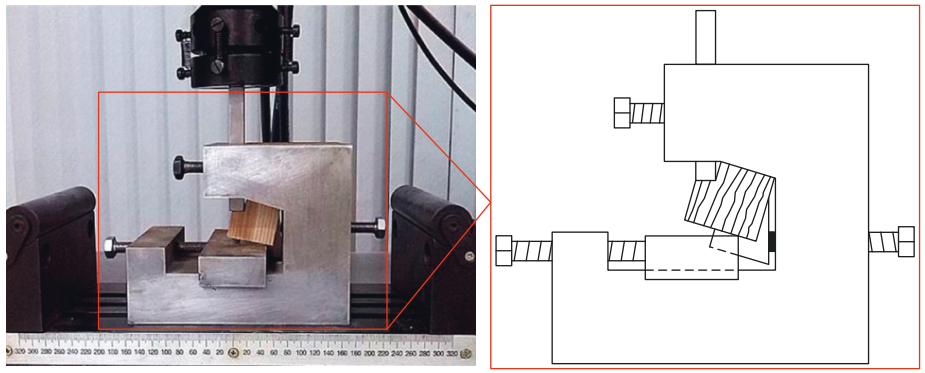

Figure 6: Load machine and ancillary equipment for the shearing test.

to grain adjusted to water content of 12% and ω is the tested water level of wood specimens.

3. Results and Discussion

In this section, evaluated physical properties (weight loss and color change) and mechanical properties (compressive strength parallel to grain, tensile strength parallel to grain, and shear stress parallel to grain) at elevated temperatures are discussed. Furthermore, comparison of mechanical properties among Chinese Dahurian larch wood to that of data obtained from many classical researches is presented.

3.1. Physical Properties

3.1.1. Weight Loss. The variation of wood weight and appearance with temperature and exposure time can provide useful references for the postdisaster analysis, which covers how serious the wood is affected by the fire and for the performance assessment on the damaged structure.

The weight loss rate of specimens in Test 1 under different temperatures and exposure times is shown in Figure 7. As can been seen, the weight loss rate of each specimen is not that obvious when the temperature retains 100°C and 200°C under the same exposure time and the weight loss is mainly caused by severe dehydration. Taking the 45 min exposure time, for example, the weight loss rate reaches 3.3% and 3.52%, respectively. Nevertheless, when temperature reaches 250°C, the weight loss rate increases significantly. Also for the 45 min exposure time, the weight loss rate reaches as high as 7.84%, which is about 2.2 times as high as that of 200°C. The reason is that wood suffers from the pyrolytic reaction, which usually happens at 200–250°C. Wood pyrolysis can be divided into two stages: cellulose pyrolysis and lignin decomposition. The first stage is characterized by rapid weight loss of cellulose and the second stage by slow pyrolysis of lignin. Wood pyrolysis speeds up when the temperature reaches 250°C, at which the moisture evaporates almost completely. Meanwhile, small molecules of gas and macromolecules of the condensable volatile component generated from pyrolysis will cause apparent weight loss.

Under the same temperature, the wood loss rate also gradually increases with the increase of temperature exposure time. When the temperature fails to reach the temperature that the wood pyrolysis requires, its exposure time has a significant effect on the weight loss rate. For instance, when the exposure time increases from 5 min to 45 min, an 80% increase of the weight loss rate of wood occurs at 100 °C. But when the temperature increases to values above the wood pyrolysis temperature, its exposure time has little impact on the weight loss rate. It can easily be seen from Figure 4 that the weight loss rate only increases by 21% at 250°C as time increases from 15 min to 45 min. This is because most of the weight loss has been done in a short period of time. Through the above analysis, conclusions can be drawn that the weight loss of wood increases with the increase of exposure temperatures and exposure time.

3.1.2. Color Change. Figure 8 illustrates the effect of temperature on the color of specimens in Test 3 (exposure time = 45 min). It can be seen that wood presents a light brown color after 100°C and 200°C treatment, showing no significant change compared with untreated specimens. However, after 250°C, the wood color turns into dark brown, showing obvious differences from the untreated specimens, which indicates that 200–250°C is a critical temperature for significant change of the wood color. Reason lies in that the lignin and hemicellulose of wood will degrade under the action of high temperature. With the increase of exposure temperature and exposure time, degradation of the cellulose and hemicellulose polysaccharide substance will take place, resulting in generation of more carbonyl and carboxyl, which eventually makes the wood color gradually change from brown to dark brown.

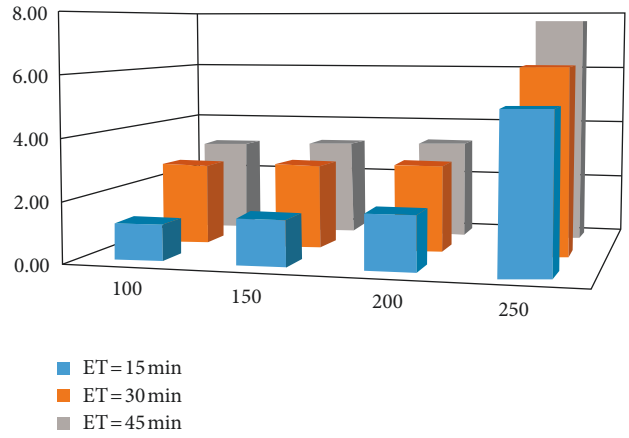

Figure 7: Weight loss rate of specimens using the natural cooling method in Test 1 ("ET" indicates the exposure time).

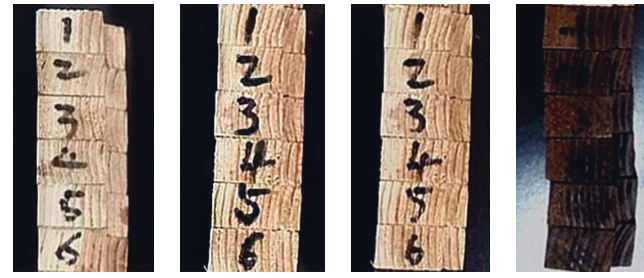

Figure 8: Effect of temperature on the wood color: (a) room temperature; (b) 100°C; (c) 200°C; (d) 250°C.

3.2. Mechanical Properties

3.2.1. Compressive Strength Parallel to Grain. Figure 9 presents the evolution of the mechanical strength parallel to grain with different exposure times of elevated temperatures under both natural and water cooling methods, which is also compared with test results obtained from Schaffer [24], Lie [25], Thomas [27], and Konig and Walleij [28]. Exposure to elevated temperatures caused degradation in the strength of wood [4]. For specimens in Test 1, the failure load in compression parallel to grain was used to evaluate the longitude compressive strength at each exposure temperature.

$\lambda_{\text{compressive}}$ is the ratio of the compressive strength $f_{c12,NC,\theta}$ and $f_{c12,WC,\theta}$ (at θ temperature) to compressive strength $f_{c12,R}$ (at room temperature) (5). The subscript "R" represents the "room temperature". $\lambda_{\text{compressive}}$ can usually be used to appreciate the variation magnitude of mechanical properties at elevated temperatures [34]:

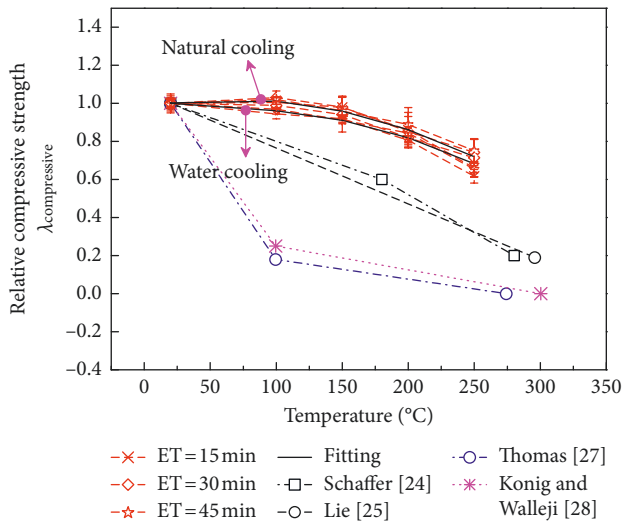

Figure 9: Relative compressive strength of wood parallel to grain as a function of exposure temperature (ET = exposure time).

$$\lambda_{compressive} = \begin{cases} \dfrac{f_{c12,NC,\theta}}{f_{c12,R}}, & \text{for natural cooling,} \\ \dfrac{f_{c12,WC,\theta}}{f_{c12,R}}, & \text{for water cooling.} \end{cases} \quad (5)$$

Seen from Figure 9, $\lambda_{compressive}$ of both this study and Schaffer [24], Lie [25], Thomas [27], and Konig and Walleij [28] basically decrease with the increase of temperature; however, there is a difference in the decline degree. Thomas [27] and Konig and Walleij [28] used the bilinear model to describe the degradation of compressive strength, where the turning point is at 100°C. The turning point of the Schaffer [24] model is at 200°C and shows a slower evolution. $\lambda_{compressive}$ changes gradually from the room temperature to 150°C, and the variation is less than 5% for both 15 min, 30 min, and 45 min exposure time, which clearly indicates that the exposure time has almost no effect on the parallel to grain compressive strength in the temperature interval of 20–150°C. It can also be seen that $\lambda_{compressive}$ decreases with the increase of temperature from 150°C to 250°C and the relative residual compressive strength decreases faster with the increasing exposure time.

It is found from this figure that when the exposure temperatures are lower than 150°C, the exposure time almost has no effect on the relative compressive strength parallel to grain. When the exposure temperatures are 200°C and 250°C, the relative compressive strength decreases greatly with the increase of exposure time.

It can be seen from Figure 9 that the residual compressive strength of specimens subjected to different temperatures with water cooling has similar evolution rules as that with natural cooling and their values are generally lower than that of the latter.

3.2.2. Tensile Strength Parallel to Grain. The relative tensile strength parallel to grain of wood expressed in $\lambda_{tensile}$ is shown in Figure 10. $\lambda_{tensile}$ is the ratio of the compressive strength $f_{t12,NC,\theta}$ and $f_{t12,WC,\theta}$ (at θ temperature) to the value of compressive strength $f_{t12,R}$ (at room temperature), as shown in the following equation:

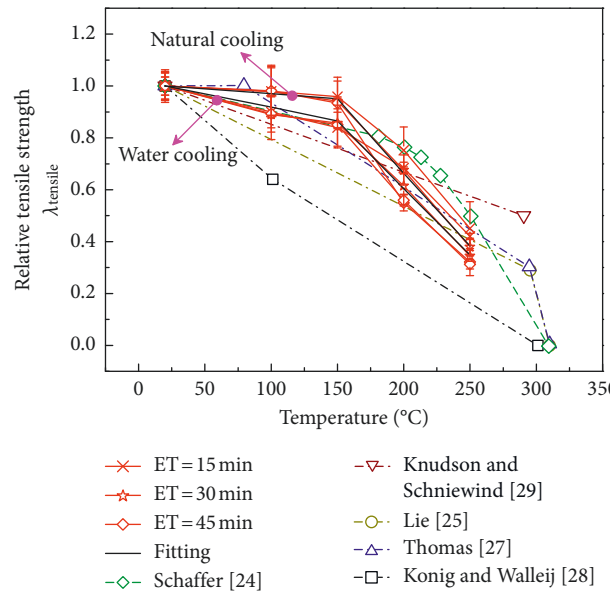

Figure 10: Relative tensile strength parallel to grain as a function of exposure temperature (ET = exposure time).

$$\lambda_{tensile} = \begin{cases} \dfrac{f_{t12,NC,\theta}}{f_{t12,R}}, & \text{for natural cooling,} \\ \dfrac{f_{t12,WC,\theta}}{f_{t12,R}}, & \text{for water cooling.} \end{cases} \quad (6)$$

The tensile strength decreases with the temperature increase (Figure 10), where the tensile strength gradually descends in the temperature range 20–150°C and then decreases rapidly when the temperature exceeds 150°C. This phenomenon is caused by the formation, evolution, and expansion of microdrawbacks in the specimens after exposure to high temperatures. The residual tensile strength of specimens with exposure times of 30 min and 45 min decrease more seriously than that of specimens with exposure time of 15 min. For any given exposure temperature, the relative tensile strength of the specimen with the exposure time of 45 min is lower than that of specimen with the exposure time of 30 min, which is also lower than that of specimen with the exposure time of 15 min.

Similar to the compressive condition, the comparison of tensile test results in this study with that from the other researchers [24, 25, 27–29] is also illustrated in Figure 10. An overall decreasing trend can be clearly seen with the increase of the exposure temperature. The calculated relative tensile strength by the authors is decreasing along a typical bilinear path with the turning temperature of 150°C. The decreasing path calculated by Konig and Walleij [28] is basically a straight line, indicating a more rapid decrease of tensile strength at elevated temperature compared with that of

other researches. According to Schaffer [24], Lie [25], and Thomas [27], the tensile strength decreases along the similar path.

Figure 10 also shows a variation of the relative tensile strength parallel to grain $\lambda_{tensile}$ with the exposure time for specimens with natural cooling and water cooling. Exposure time almost has no effect on the relative tensile strength parallel to grain, especially for the temperature range of 20°C–150°C. The relative tensile strength of the specimens with the higher exposure temperature is higher than that of specimens with the lower exposure temperature for any exposure time.

It can be seen from Figure 10 that the residual tensile strength of specimens subjected to different temperatures with water cooling have similar evolution rules as that with natural cooling and their values are generally lower than that of the latter.

3.2.3. Shear Strength Parallel to Grain. Figure 11 shows variation of relative shear strength parallel to grain λ_{shear} under different exposure temperatures. λ_{shear} is the ratio of the shear strength $f_{s12,NC,\theta}$ and $f_{s12,WC,\theta}$ (at θ temperature) on the value $f_{s12,R}$ (at room temperature), as shown in the following equation:

$$\lambda_{shear} = \begin{cases} \dfrac{f_{s12,NC,\theta}}{f_{s12R,}}, & \text{for natural cooling,} \\ \dfrac{f_{s12,WC,\theta}}{f_{s12,R}}, & \text{for water cooling.} \end{cases} \quad (7)$$

It is found from Figure 11 that the residual shear strength parallel to grain of specimens after elevated temperatures of 100°C and 150°C is slightly lower than that of the specimen at room temperature and then decreases significantly when the exposure temperature increases. The exposure time almost has no effect on the relative shear strength parallel to grain.

The relative shear strength of wood parallel to grain, which can be conveniently used to evaluate the magnitude of the variation according to the exposure temperature and cooling methods, is presented in Figure 11. It can be seen that the shear strength parallel to grain is experiencing a slight decrease from the room temperature up to 150°C, with a fast reduction between 150°C and 250°C. Residual tensile strength of specimens subjected to water cooling is generally lower than that to natural cooling.

4. Degradation Model of Wood Strength after High-Temperature Exposure

The material properties measured at elevated temperatures usually give physical constants in the form of mathematical equations that can be used as mathematical models for the fire resistance calculations of structures [34, 35]. From another point of view, such formulas constitute degenerate models for the mechanical properties of materials. The employ of these expressions lays the basis for the prediction of fire resistance ratings of structures to a great extent. To

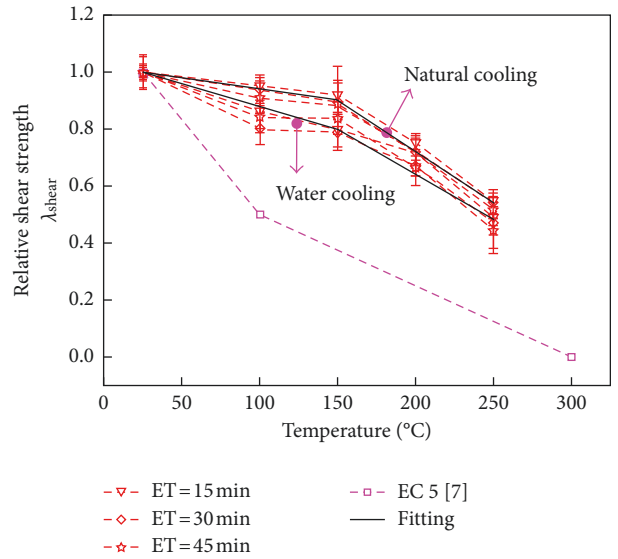

Figure 11: Variation of relative residual shear strength parallel to grain with temperature and cooling methods (ET = exposure time).

make material strength properties independent variables, the degradation models of wood mechanical properties proposed here are expressed empirically by giving the relations between the relative compressive strength parallel to grain, relative tensile strength parallel to grain, and relative shear strength parallel to grain and the elevated exposure temperature range of 20–250°C and exposure time range of 15–45 min. Based on the test results conducted in this study, the least square fitting analysis is realized for using convenience by means of software Origin 9.0.

The proposed models describing the degradation of compressive strength, tensile strength, and shear strength parallel to grain are clearly given in Table 2. Good correspondence was obtained with the experimental data, as shown in Figures 9–11.

5. Damage Constitutive Model (CDM) of Wood after High-Temperature Exposure

Finite-element simulation has become an increasingly used method to evaluate the healthy condition of structures. For analysis accuracy of fire-damaged wooden structures, the mechanical properties of fire-damaged wood materials are of great significance, of which the most important is the stress-strain relationships.

Reasonable constitutive model must consider the factors of exposure temperature and exposure time simultaneously. Compressive damage constitutive model (CDM_C) and tensile damage constitutive model (CDM_T) parallel to grain after high-exposure temperature with different time ranges were proposed, respectively, within the framework of damage mechanics.

Scalar damage variable D is introduced to reflect the damage condition of wood at the elevated temperature, which can be defined as the relative reduction of the pressed area perpendicular to the loading direction:

Table 2: Degradation model of high temperature unstressed material property relationships for wood.

Material property	Relation
Compressive strength parallel to grain	$\lambda_{\text{compressive}} = \begin{cases} 1, & T = 20^{\circ}\text{C, natural and water cooling,} \\ -9 \times 10^{-6}T^2 + 0.0012T + 0.982, & T > 20^{\circ}\text{C, natural cooling,} \\ c_c \cdot (-9 \times 10^{-6}T^2 + 0.0012T + 0.982), & T > 20^{\circ}\text{C, water cooling,} \end{cases}$
Tensile strength parallel to grain	$\lambda_{\text{tensile}} = \begin{cases} 1, & T = 20^{\circ}\text{C, natural and water cooling,} \\ -0.0004T + 1.015, & 20^{\circ}\text{C} < T \le 150^{\circ}\text{C, natural cooling,} \\ c_t \cdot (-0.0004T + 1.015), & 20^{\circ}\text{C} < T \le 150^{\circ}\text{C, water cooling,} \\ -0.0056T + 1.786, & 150^{\circ}\text{C} < T \le 250^{\circ}\text{C, natural cooling,} \\ c_t \cdot (-0.0056T + 1.786), & 150^{\circ}\text{C} < T \le 250^{\circ}\text{C, water cooling,} \end{cases}$
Shear strength parallel to grain	$\lambda_{\text{shear}} = \begin{cases} 1, & T = 20^{\circ}\text{C, natural and water cooling,} \\ -0.0008T + 1.021, & 20^{\circ}\text{C} < T \le 150^{\circ}\text{C, natural cooling,} \\ c_\tau \cdot (-0.0008T + 1.021), & 20^{\circ}\text{C} < T \le 150^{\circ}\text{C, water cooling,} \\ -0.0036T + 1.441, & 150^{\circ}\text{C} < T \le 250^{\circ}\text{C, natural cooling,} \\ c_\tau \cdot (-0.0036T + 1.441), & 150^{\circ}\text{C} < T \le 250^{\circ}\text{C, water cooling,} \end{cases}$

Note: $c_{c=0.95}$, $c_{t=0.91}$ and $c_{\tau=0.89}$ represent the cooling method coefficient for compressive strength, tensile strength and shear strength.

Table 3: CDM of wood at elevated temperature.

CDM	Relation
CDM_C	$\sigma = E_0 \cdot (1 - D_{\text{compressive}}) \cdot \varepsilon \cdot \lambda_{\text{compressive}}$ $D_{\text{compressive}} = \begin{cases} 0, & 0 \le \varepsilon \le \varepsilon_e, \\ 1 - (a_0/\varepsilon) - a_1 - a_2\varepsilon - a_3\varepsilon^2, & \varepsilon > \varepsilon_e, \end{cases}$ $\varepsilon_e = 0.01067 + 5.57 \times 10^{-5}T + 1.44 \times 10^{-4}t - 1.79 \times 10^{-6}T \cdot t$
CDM_T	$\sigma = E_0 \cdot (1 - D_{\text{tensile}}) \cdot \varepsilon \cdot \lambda_{\text{tensile}}$ $D_{\text{tensile}} \equiv 0$

$$D = \frac{(A - A_e)}{A}, \tag{8}$$

where A is the original area of the material and A_e is the effective area of wood after exposure to high temperature.

For the damaged material, the measurement of an effective area is difficult. As an indirect method, the strain equivalence principle is used to obtain the constitutive model of the damaged material:

$$\sigma = E(1 - D)\varepsilon. \tag{9}$$

The concrete expression of D depends on the material used and the interstress state. The proposed damage constitutive models describe the evolution of the compressive and tensile.

Stress-strain relationships parallel to grain are clearly shown in Table 3. D_{tensile} and $D_{\text{compressive}}$ denote the tensile and compressive damage variables, respectively.

The expressions of a_0, a_1, a_2, and a_3 are exposure temperature T and exposure time t dependent variables and can be determined according to the test results, shown as follows:

$$\begin{aligned} a_0 &= 0.0072 - 9.66 \times 10^{-5}T - 1.64 \times 10^{-4}t + 2.39 \times 10^{-6}T \cdot t, \\ a_1 &= 1.585 + 8.49 \times 10^{-4}T - 7.53 \times 10^{-3}t - 4.57 \times 10^{-5}T \cdot t, \\ a_2 &= 0.061T + 0.668t - 1.64 \times 10^{-3}T \cdot t - 47.34, \\ a_3 &= 429.89 - 1.126T - 8.785t + 0.028T \cdot t. \end{aligned} \tag{10}$$

The established constitutive model (CDM_C and CMD_T) was compared with the test results conducted in this studies (Figure 12). It can be seen that the overall compressive and tensile behaviors parallel to grain of the wood material after high-exposure temperature and exposure time are well simulated by the CDM_C and CMD_T using the natural cooling method.

6. Conclusions

The influences of exposure temperature (100, 150, 200, and 250°C), exposure time (15, 30, and 45 min), and cooling method (natural cooling and water cooling) on the residual strength (compressive, tensile, and shear strength) of wood parallel to grain after elevated temperature were investigated in this paper. Based on analysis of the test results, the following conclusions can be drawn:

(1) Exposure temperature has a great impact on the weight loss and color change of wood: with the increase of temperature and the exposure time, an increase in weight loss can be observed, and the wood color changed from light brown to dark brown. 200°C~250°C is a critical temperature range that contributes to the weight loss and color change of wood.

(2) Various mechanical properties of wood suffer different degradations after exposure to high temperatures. The descend gradient is affected by exposure

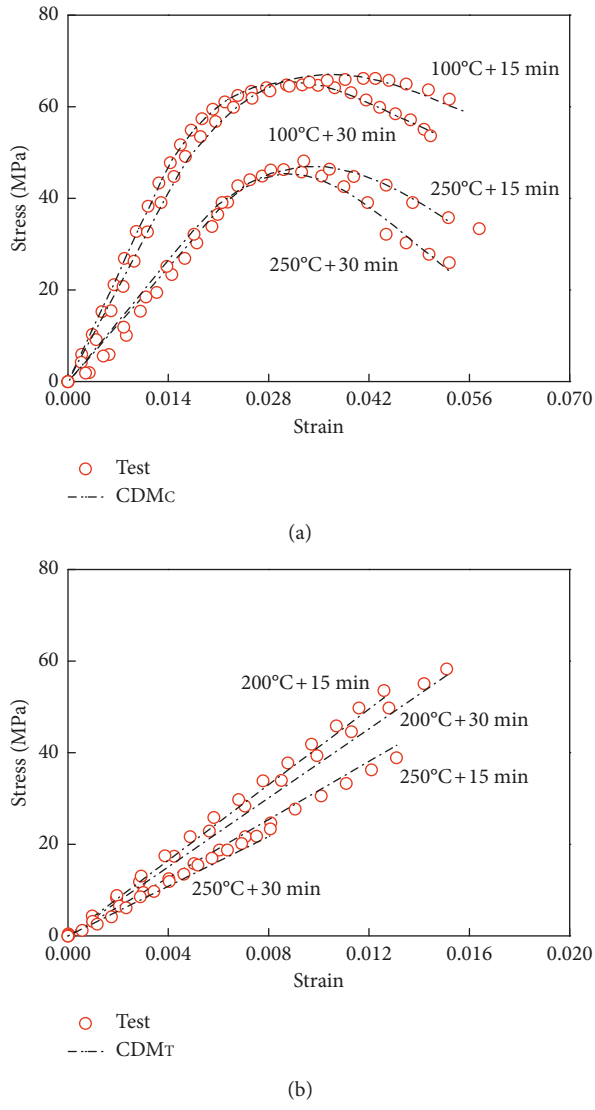

Figure 12: Stress-strain relationship of wood after high-exposure temperature when using natural cooling: (a) compressive condition; (b) tensile condition.

temperature, exposure time, and cooling method, but mainly by exposure temperature.

(3) The residual compressive strength and shear strength parallel to grain of specimens after the elevated temperatures of 100°C and 150°C are slightly higher than that of the specimen at the room temperature. The residual tensile strength parallel to grain of specimens after elevated temperatures of 100°C and 150°C is almost to that of the specimen at the room temperature. Then, all of the three strength decreases significantly when the exposure temperature increases.

(4) For any given exposure temperature, the relative compressive strength and tensile strength of the specimens with the exposure time of 45 min are lower than that with the exposure time of 30 min, which are also lower than that of 15 min. But exposure time almost has no effect on the relative shear strength parallel to grain.

(5) The residual compressive strength, tensile strength, and shear strength of specimens with water cooling are slightly lower than that with natural cooling.

Data Availability

All data analysed during this study are included in this article.

Conflicts of Interest

The authors declare that they have no conflicts of interest.

Acknowledgments

The authors of this paper gratefully acknowledge the funding support received from the National Natural Science Foundation of China (Grant no. 51878550), the National Key Research and Development Program of China (Grant no. 2017YFC0703507), Shaanxi Provincial Government (2014SZS04-P04), and Science and Technology Department of Shaanxi Province of China (Grant no. 2016ZDJC-23). Gratitude is also extended to all members of the Structural Engineering Laboratory of XAUAT.

References

[1] X. Li, J. Zhao, G. Ma, and W. Chen, "Experimental study on the seismic performance of a double-span traditional timber frame," *Engineering Structures*, vol. 98, pp. 141–150, 2015.

[2] S. M. Cramer and R. H. White, *Fire Performance Issues*, American Society of Civil Engineers (ASCE), Reston, VA, USA, 1997.

[3] GB 50165, *Technical Code for Maintenance and Strengthening of Ancient Timber Buildings*, Ministry of Construction of the People's Republic of China, Beijing, China, 1992, in Chinese.

[4] A. Sinha, "Thermal degradation modeling of flexural strength of wood after exposure to elevated temperatures," *Wood Material Science and Engineering*, vol. 8, no. 2, pp. 111–118, 2013.

[5] J. Heitz, *Fire Resistance in American Heavy Timber Construction*, Springer Nature, Basel, Switzerland, 2016.

[6] A. H. Buchanan, *Structural Design for Fire Safety*, John Wiley and Sons, West Sussex, England, 2002.

[7] Eurocode 5, *Design of Timber Structures-Part 1-1: General Rules and Rules for Buildings (EN 1995-1-1:2004+A2:2014)*, European Committee for Standardization, Brussels, Belgium, 2003.

[8] O. Kai, "Fire resistance of wood structures," *Fire Technology*, vol. 21, no. 1, pp. 34–40, 1985.

[9] J. M. Njankouo, J. C. Dotreppe, and J. M. Franssen, "Experimental study of the charring rate of tropical hardwoods," *Fire and Materials*, vol. 28, no. 1, pp. 15–24, 2004.

[10] J. Zhang, Z. H. Liu, Y. X. Xu, S. W. Ma, and Q. F. Xu, "An experimental and numerical study on the charring rate of timber beams exposed to three-side fire," *Scientia Sinica Technologica*, vol. 55, no. 12, pp. 3434–3444, 2012.

[11] R. H. White and E. V. Nordheim, "Charring rate of wood for ASTM E 119 exposure," *Fire Technology*, vol. 28, no. 1, pp. 5–30, 1992.

[12] A. Firmanti, B. Subiyanto, and S. Takino, "The critical stress in various stress levels of bending member on fire exposure for mechanically graded lumber," *Journal of Wood Science*, vol. 50, no. 5, pp. 385–390, 2004.

[13] Q. F. Xu, X. M. Li, J. Zhang, B. G. Mu, and Q. Xu, "Experimental study of the mechanical behavior of timber beams exposed to three-side fire," *China Civil Engineering Journal*, vol. 44, pp. 64–71, 2011, in Chinese.

[14] L. Z. Chen, X. Wang, and Q. F. Xu, "Calculation methods for fire rate of timber beams exposed to three-side fire," *Journal of Disaster Prevention and Mitigation Engineering*, vol. 36, pp. 399–404, 2016, in Chinese.

[15] L. L. Wen, L. Y. Han, H. B. Zhou, and C. J. Zhuge, "Developing charring rate models for Chinese species based on the thermodynamic theory," *Wood Science and Technology*, vol. 51, no. 5, pp. 1117–1131, 2017.

[16] B. A. L. Östman, "Wood tensile strength at temperatures and moisture contents simulating fire conditions," *Wood Science and Technology*, vol. 19, no. 2, pp. 103–116, 1985.

[17] J. E. Winandy and P. K. Lebow, "Kinetics models for thermal degradation of strength of fire-retardant treated wood," *Wood and Fiber Science*, vol. 28, pp. 39–52, 1996.

[18] P. Bekhta and P. Niema, "Effect of high temperature on the change in color, dimensional stability and mechanical properties of spruce wood," *Holzforschung*, vol. 57, no. 5, pp. 539–546, 2003.

[19] I. M. V. Zeeland, J. J. Salinas, and J. R. Mehaffey, "Compressive strength of lumber at high temperatures," *Fire and Materials*, vol. 29, no. 2, pp. 71–90, 2005.

[20] T. Goodrich, N. Nawaz, S. Feih, B. Y. Lattimer, and A. P. Mouritz, "High-temperature mechanical properties and thermal recovery of balsa wood," *Journal of Wood Science*, vol. 56, no. 6, pp. 437–443, 2010.

[21] G. Hall, *Fire Resistance Tests of Laminated Timber Beams*, Timber Research and Development Association, High Wycombe, UK, 1968.

[22] L. F. Li, "Numerical analysis of the fire resistance of post-beam timber frame," Dissertation, Southeast University, Nanjing, China, 2014.

[23] R. Preusser, "Plastic and elastic behaviour of wood affected by heat in open systems," *Holztechnologie*, vol. 9, no. 4, pp. 229–231, 1968.

[24] E. L. Schaffer, *Elevated temperature effect on the longitudinal mechanical properties of wood*, Ph.D. dissertation, University of Wisconsin System, Madison, WI, USA, 1970.

[25] T. T. Lie, *Structural Fire Protection*, American Society of Civil Engineers, New York, NY, USA, 1992.

[26] M. L. Janssens, "Thermo-physical properties for wood pyrolysis models," in *Proceedings of Pacific Timber Engineering Conference*, Gold Coast, Australia, July 1994.

[27] G. C. Thomas, *Fire resistance of light timber framed walls and floors*, Ph.D. dissertation, University of Canterbury, Christchurch, New Zealand, 1997.

[28] J. Konig and L. Walleij, *Timber Frame Assemblies Exposed to Standard and Parametric Fires: Part 2: A Design Model for Standard Fire Exposure*, Rapport Institutet for Trateknisk Forskning, Stockholm, Sweden, 2000.

[29] R. M. Knudson and A. P. Schniewind, "Performance of structural wood members exposed to fire," *Forest Products Journal*, vol. 25, no. 2, pp. 23–32, 1975.

[30] GB 1929-91, *Method of Sample Logs Sawing and Test Specimens Selection for Physical and Mechanical Tests of Wood*, Ministry of Housing and Urban-Rural Development of the People's Republic of China, Beijing, China, 1991, in Chinese.

[31] GB 1935-91, *Method of Testing in Compressive Strength Parallel to Grain of Wood*, Ministry of Housing and Urban-Rural Development of the People's Republic of China, Beijing, China, 1991, in Chinese.

[32] GB 1938-91, *Method of Testing in Tensile Strength Parallel to Grain of Wood*, Ministry of Housing and Urban-Rural Development of the People's Republic of China, Beijing, China, 1991, in Chinese.

[33] GB 1937-91, *Method of Testing in Shearing Strength Parallel to Grain of Wood*, Ministry of Housing and Urban-Rural Development of the People's Republic of China, Beijing, China, 1991, in Chinese.

[34] W. Khaliq and M. F. Bashir, "High temperature mechanical and material properties of burnt masonry bricks," *Materials and Structures*, vol. 49, no. 12, pp. 1–14, 2016.

[35] J. C. Bidoung, P. Pliya, P. Meukam, A. Noumowé, and T. Beda, "Behaviour of clay bricks from small-scale production units after high temperature exposure," *Materials and Structures*, vol. 49, no. 12, pp. 1–16, 2016.